Available online at www.sciencedirect.com
ScienceDirect
Journal of Nuclear Materials 374 (2008) 453–460
journal of nuclear materials
www.elsevier.com/locate/jnucmat

Reliability analysis of dispersion nuclear fuel elements

Shurong Ding [a,*], Xin Jiang [a], Yongzhong Huo [a,*], Lin an Li [b]

[a] Department of Mechanics and Engineering Science, Fudan University, Shanghai 200433, PR China
[b] Department of Mechanics, Tianjin University, Tianjin 300072, PR China

Received 18 April 2007; accepted 25 October 2007

Abstract

Taking a dispersion fuel element as a special particle composite, the representative volume element is chosen to act as the research object. The fuel swelling is simulated through temperature increase. The large strain elastoplastic analysis is carried out for the mechanical behaviors using FEM. The results indicate that the fission swelling is simulated successfully; the thickness increments grow linearly with burnup; with increasing of burnup: (1) the first principal stresses at fuel particles change from tensile ones to compression ones, (2) the maximum Mises stresses at the particles transfer from the centers of fuel particles to the location close to the interfaces between the matrix and the particles, their values increase with burnup; the maximum Mises stresses at the matrix exist in the middle location between the two particles near the mid-plane along the length (or width) direction, and the maximum plastic strains are also at the above region.

1. Introduction

Dispersion fuel elements [1] are solid nuclear fuels used in nuclear reactors distinguished by having a fissionable material (such as compounds of uranium or plutonium, etc.) dispersed as small particles through a non-fissionable matrix of metal, ceramic or graphite, which are similar to particle-reinforced composites in the configurations.

The basic thought of dispersion fuels is to separate the fuel particles from the matrix material. When the majority of matrix is not damaged by the fission products, the fuel particles might be surrounded and restricted. Good thermal conductivity performance might be kept and higher burnup might be achieved than the big block fuels (such as the traditional pellet-type fuels). Due to their high burnup and thermal conductivity, dispersion fuel elements are widely used in the research and test reactors and nuclear power reactors.

Nuclear wastes bring great challenge to science, technology and engineering. The European Unions and American are engaged in carrying out research on making use of dispersion fuel types [2,3] to dispose nuclear wastes.

Nuclear fissions of fuel particles produce fission heat [4,5]; and the solid and inert gas fission products brought by nuclear fission might lead to volume swelling of fuel particles with increasing of burnup, moreover, fission gas release might occur [6–9]. Furthermore, the fission products and high energy ions produced by nuclear fissions might make the mechanical behaviors of the matrix materials change with burnup [10]. In order to realize high power, the volume loading of fuel particle in the dispersion fuels will have to achieve 50%. As a result, the amount of fuel particles contained in the dispersion fuel plates generally may reach 10^8–10^9. Adding to the complexities mentioned above, the fuel particles are not evenly distributed, which makes the structures of dispersion fuels very complicated and further increases the research difficulty.

The important application of dispersion fuels in the aspects of country economy and nuclear wastes with heavy radioactivity, the internal demanding environment and the

* Corresponding authors.
E-mail addresses: dsr1971@163.com (S. Ding), yzhuo@fudan.edu.cn (Y. Huo).

0022-3115/$ - see front matter © 2007 Elsevier B.V. All rights reserved.
doi:10.1016/j.jnucmat.2007.10.006

complex stress states induced by the complicated structures all make the research on dispersion fuels not only have important practicality value, but also have scientific significance.

Because the irradiation experimental research is very time-consuming, the cost is also very high and it is hard to be observed in situ, it is necessary to develop suitable theoretical models to carry out numerical simulation in order to design and create long-life dispersion nuclear fuel elements.

In the early years of 1950s and 1960s, some cursory reliability analysis [11,12] existed without allowing for the mechanical behaviors of the fuel particles and matrix. High burnup fuel behavior has been known as a key issue in terms of fuel design and reliability. And fuel design and reliability prediction is directly correlated to economic performance. It is necessary to accurately simulate the thermal–mechanical behaviors besides the experimental research. Some researches [13,14] are conducted on fuel swelling: they adopted the spherical symmetry model without considering the mutual action among fuel particles, so the obtained matrix stresses are spherical symmetrical, which could not embody the actual stress state. Lately, in order to analyze the mutual action among the fuel particles more precisely, the analysis using FEM considering more actual particle distribution is presented [3]. However, since the amount of the fuel particles is very large and the fission course is quite complex, the computation veracity and effectiveness are far from meeting the needs of the actual application. The relative research on dispersion fuel plate is limited.

In this study, considering the actual geometry of a dispersion fuel plate, the three-dimensional representative volume element is chosen to act as the research object, which might simulate not only the micro stress–strain field but also the macro deformation along the thickness. Owing to the similarity of the irradiation swelling and the thermal expansion, the fuel swelling is simulated through temperature increase during burnup. The large strain elastoplastic analysis is carried out for the thermal–mechanical behaviors using finite element method. The stress distribution is studied and the thickness and strength changes with burnup are analyzed.

2. Theoretical models

The heat emitted by nuclear fissions of fuel particles might result in the temperature variation of dispersion fuels and lead to appearance of thermal stresses. In order to obtain thermal stresses, the temperature field should be determined firstly.

For steady-state thermal analysis problems, the thermal conductivities of the fuel particles and matrix, the fission rates of the fuel particles, the temperature of the periphery fluid, the heat transfer coefficient between the matrix and the periphery fluid will all affect the temperature distributions of fuel elements.

2.1. Heat conduction analysis model

2.1.1. Heat conduction equation and boundary conditions

The equation of heat conduction for steady-state is given as

$$k\nabla^2 T + \dot{q} = 0, \tag{1}$$

where k is the thermal conductivity, T is the temperature, $\dot{q}$ is the heat generation rate.

In order to determine the temperature field of dispersion fuel elements, firstly the boundary condition of the problem, the thermal conductivities of the particles and matrix and the heat generation rate of fuel particles should be determined.

The three kinds of boundary conditions are as follows:

$$T = g(x, y, z), \tag{2}$$

$$-k\frac{\partial T}{\partial n} = f(x, y, z), \tag{3}$$

$$-k\frac{\partial T}{\partial n} = h(T - T_f), \tag{4}$$

where Eq. (2) describes that the boundary temperature is known, Eq. (3) depicts that the thermal flux of the specified boundary is given. Eq. (4) denotes the condition of the heat transfer boundary should be met; where h means the heat transfer coefficient, T_f expresses the temperature of the periphery fluid, n represent the external normal direction of the boundary surface.

2.1.2. The thermal conductivities of the fuel particles and the matrix

For UO_2 particles, Lucuta et al. [15] developed the model of thermal conductivities, in which the effects of temperature, burnup, porosity and fission products on the thermal conductivity are comprehensively considered. The model is suitable to the high burnup circumstances.

$$k_0 = \frac{1}{0.0375 + 2.165 \times 10^{-4} T} + \left[\frac{4.715 \times 10^9}{T^2}\right] \exp\left(-\frac{16361}{T}\right), \tag{5}$$

where Eq. (5) denotes the thermal conductivity of un-irradiated and dense UO_2, which is proposed by Harding and Martin (1989). k_0 (W/m K) is the thermal conductivity and T (K) is the temperature.

$$\mathrm{FD} = \left[\frac{1.09}{B^{3.265}} + \frac{0.0643}{\sqrt{B}}\sqrt{T}\right] \arctan\left[\frac{1}{\frac{1.09}{B^{3.265}} + \frac{0.0643}{\sqrt{B}}\sqrt{T}}\right], \tag{6}$$

$$\mathrm{FP} = 1 + \left[\frac{0.019B}{3 - 0.019B}\right]\left[\frac{1}{1 + \exp(-\frac{T-1200}{100})}\right]. \tag{7}$$

FD and FP reflect the effect factors of the dissolved and precipitated fission products on the thermal conductivities, respectively, where B denotes burnup (at.%), T(K) depicts the temperature.

$$\mathrm{FM} = \frac{1-P}{1+(s-1)P}. \tag{8}$$

FM expresses the effect of porosity. In Eq. (8) P (%) describes the porosity fraction, s denotes the shape factor for pores ($s = 1.5$ for spherical pores).

$$\mathrm{FR} = 1 - \frac{0.2}{1+\exp(\frac{T-900}{80})}, \tag{9}$$

where FR gives the effect of the irradiation effect and T (K) denotes the temperature.

Based on the above expressions, the thermal conductivity of irradiated UO_2 is given as

$$k = k_0 \cdot \mathrm{FD} \cdot \mathrm{FP} \cdot \mathrm{FM} \cdot \mathrm{FR}. \tag{10}$$

For the Zircaloy matrix, its thermal conductivity from the room temperature to the melting point can be described as [16]

$$k = 7.51 + 2.09 \times 10^{-2} T - 1.45 \times 10^{-5} T^2 + 7.67 \times 10^{-9} T^3. \tag{11}$$

2.1.3. The computation of heat generation rate

The heat generation rates of fuel particles are corresponding to their fission rates. For a certain fission rate, considering that the emitted quantity of heat by one time fission is 200 Mev and 1 ev equals 1.602×10^{-19} J, thus the corresponding heat generation rate can be worked out.

2.2. The constitutive model

In order to precisely simulate the mechanical behaviors of dispersion fuels, the material models reflecting the in-pile behaviors should be adopted.

2.2.1. The constitutive model of fuel particles

The total deformation increment consists of the components of elasticity, plasticity, swelling and the thermal one,

$$\mathrm{d}\varepsilon^{\mathrm{e}} = \mathrm{d}\varepsilon - \mathrm{d}\varepsilon^{\mathrm{th}} - \mathrm{d}\varepsilon^{\mathrm{sw}} - \mathrm{d}\varepsilon^{\mathrm{p}}, \tag{12}$$

where the superscript e denotes the elastic strain increment and the superscript th denotes the thermal strain one, sw describes the swelling and p expresses the plastic strain increment.

The thermal strain increment is given by

$$\left\{\mathrm{d}\varepsilon^{\mathrm{th}}\right\} = \Delta T[\,\alpha_x \quad \alpha_y \quad \alpha_z \quad 0 \quad 0 \quad 0\,]^{\mathrm{T}}, \tag{13}$$

where ΔT(K) is the temperature change, α_x, α_y, α_z denote the thermal expansion coefficients along X, Y and Z directions.

The thermal expansion of UO_2 fuel particles can be expressed as [17]

$$\Delta l/l = -3.0289 \times 10^{-4} + 8.4217 \times 10^{-6} T + 2.1481 \times 10^{-9} T^2, \tag{14}$$

where T (°C) denotes temperature. The application range of the above equation is from 27 °C to 1260 °C and $\Delta l/l$ is the linear thermal expansion relative to the length at 27 °C.

The elastic modulus of UO_2 fuel particles can be described as [16]

$$E = 2.26 \times 10^{11}(1 - 1.131 \times 10^{-4} T)[1 - 2.62(1-D)], \tag{15}$$

where E is the elastic modulus, whose unit is Pa. T is the temperature, whose unit is °C and D is the theory density (92–98%).

The Mises hardening rule of UO_2 fuel particles is as the following [17]:

$$\bar{\sigma} = \begin{cases} 66.9 - 0.0397 \cdot T + (520.0 - 0.386 \cdot T) \cdot \bar{\varepsilon}_p, & T \leqslant 1200\,^{\circ}\mathrm{C} \\ 36.6 - 0.0144 \cdot T + (139.5 - 0.06875 \cdot T) \cdot \bar{\varepsilon}_p, & T \geqslant 1200\,^{\circ}\mathrm{C}, \end{cases} \tag{16}$$

where $\bar{\sigma}$ is the Mises equivalent stress, whose unit is kgf/mm^2; $\bar{\varepsilon}_p$ is the equivalent plastic strain.

2.2.2. The material model of the matrix

The thermal expansion coefficient [16] is 5.5e − 6/°C. Young's modulus and Possion's ratio of the Zircaloy matrix adopt Fisher Model [18]:

$$E = [9.9 \times 10^5 - 566.9 \times (T - 273.15)] \times 9.8067 \times 10^4, \tag{17}$$

where E is Young's modulus (Pa), T is temperature (K).

$$\upsilon = 0.3303 + 8.376 \times 10^{-5}(T - 273.15), \tag{18}$$

where T is temperature (K).

The fast neutrons generated by fission might make the Zircaloy matrix harden and brittle.

The strain-hardening curve is described as [19]

$$\sigma = K\varepsilon^n \tag{19}$$

where σ is the true stress, ε is the true strain and n is the strain-hardening exponent.

$$K = K_{0.2\%}\left(\frac{K_{0.2\%}}{E} + 0.002\right)^{-n},$$

$$K_{0.2\%} = \sigma_y + 33.44(1 - \exp(-B\phi t))^{1/2}, \quad (\mathrm{kgf/mm^2})$$

$$B = 2.92 \times 10^{-21} \exp(1 - 1.6 \times 10^{-14}\phi)$$

$$n = 0.0504 + 0.0001435T,$$

σ_y is the yield stress, which has the following formula:

$$\sigma_y = 21.6 - 0.0213T,$$

where ϕt (n/cm^2) is the fast neutron fluence and T (°C) is the temperature and the application range of the above equations is that the expression $220 \leqslant T \leqslant 450$ °C is satisfied.

2.3. Swelling simulation equation

The total swelling of the fuel particles include three parts: gas-bubble swelling, solid fission product swelling and the densification due to the variation of the porosity.

(A) Gas-bubble swelling [20]

$$\left(\frac{\Delta V}{V}\right)^{gs} = 4.396 \times 10^2 \exp\left(-\frac{1.645 \times 10^4}{T_s}\right),$$
$$T_s = T - 100. \tag{20}$$

The above expression depicts the volume fraction of gas-bubble swelling per 10^{20}fissions/cm^3, T (K): temperature.

(B) Solid FP swelling [21]

$$\left(\frac{\Delta V}{V}\right)^{ss} = 0.0025 \approx 0.62\ \text{vol.}\%/(10\ \text{Gwd/t}). \tag{21}$$

Eq. (21) describes the volume fraction of solid FP swelling per 10^{20} fissions/cm^3.

(C) Densification of UO_2 [22]

$$\frac{\Delta V}{V} = -[0.01420(1 - \exp(-6.7943 \cdot \text{BU})) + 0.00793(1 - \exp(-1.1434 \cdot \text{BU}))] \cdot \text{ADST}, \tag{22}$$

where BU: burnup (MWD/kgUO2), ADST: adjusting factor (=0.6).

The entire load should be divided into many time steps for the large strain elastoplastic FEM. And the temperature change and swelling of fuel particle are the main loads.

Swelling of fuel particles leads to volume variation only without shape change. It is similar to thermal expansion. Owing to the similarity of the irradiation swelling and thermal expansion, the swelling is simulated through the temperature increase during burnup.

The relation between fission swelling (corresponding to different burnup) and the relative strain (corresponding to the temperature variation) should be developed.

For the fission swelling of fuel particles might reach a quite large extent, so the large strain finite element method should be used. The enough time steps should be discretized in order that the deformation increment is treated as small one.

We have

$$\frac{V_n}{V_{n-1}} = J = (1 + \Delta\varepsilon)^3 \tag{23}$$

$$\frac{V_1}{V_0} \cdot \frac{V_2}{V_1} \cdots \frac{V_n}{V_{n-1}} = (1 + \Delta\varepsilon)^{3n} \tag{24}$$

$$\frac{V_n - V_0}{V_0} = (1 + \Delta\varepsilon)^{3n} - 1 \tag{25}$$

$$n\Delta\varepsilon = \alpha\Delta T, \tag{26}$$

where V_n is the volume of time step n, $\Delta\varepsilon$ is the small swelling strain of every time step.

If the fission swelling corresponding to a certain burnup is known, according to Eq. (25) $\Delta\varepsilon$ might be determined with n large enough. Then the relation between the total swelling strain and the swelling rate is obtained. And the relative temperature change might be worked out.

3. The finite element model

According to the research thought of particle-reinforced composites [23], the relative simple instance is first considered. Assuming that the spherical particles with the diameter being 100 μm are periodically arranged in the matrix illustrated as Fig. 1, based on the periodicity and the actual geometry shape that the sizes along the length direction and the width direction are much larger than the one along the thickness with 1.27 mm, so the finite element model is selected as Fig. 2, where the plane $Z = 0$ represents the mid-plane of the fuel plate and the plane $Z = h/2$ represent the upper surface of the plate. Export path 1 locates at the line through the fuel particles from the mid-plane to the upper surface of the fuel plate. Export path 2 is the line at the mid-plane which is along the X axis. The material model of the fission fragment damage zone is assumed to be the same as the Zircaloy matrix. And the mechanical performance of irradiation-hardening and brittleness for the matrix is not considered.

The finite model is discretized as 31777 elements and 46983 nodes. In accordance with the convergence investigation, it is determined that the enough precision can be achieved.

The used boundary condition to determine the temperature field is given as

(1) $X = 0$ plane, $X = a/2$ plane, $Y = 0$ plane, $Y = a/2$ plane, $Z = 0$ plane satisfy: $-k\frac{\partial T}{\partial n} = 0$.
(2) $Z = h/2$ satisfies the convection boundary condition as Eq. (4): $-k\frac{\partial T}{\partial n} = h(T - T_f)$.
(3) The temperature of the periphery fluid T_f is 673 K.
(4) The heat transfer coefficient used is $3e^{-2}$ W/mm^2 K.

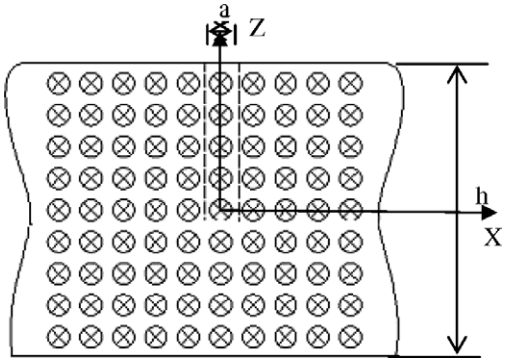

Fig. 1. The sketch map of the dispersion fuel plate.

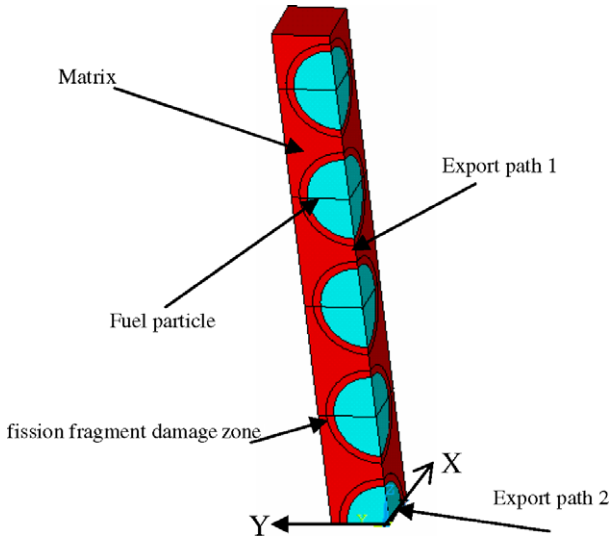

Fig. 2. The finite element model of the dispersion fuel plate.

The used boundary condition to determine the stress field is as the following:

(1) The symmetric boundary condition is applied at the planes $X = 0$, $X = a/2$, $Y = 0$, $Y = a/2$ and $Z = 0$.
(2) The continuous displacement conditions are met at the contact surfaces between the fuel particles and the matrix.

The finite element model shown as Fig. 2 denotes the fuel plate with the volume fraction of fuel particles being 20%. The developed finite element models are different depending on different particle volume fractions, particle sizes and geometries.

4. Results and discussion

Firstly, the temperature field is calculated. The fission rate of the fuel particles considered is 10^{20}fissions/m^3 s, and the fuel theory density considered is 98%. After the temperature distribution values at all the nodes are obtained, the node temperatures are introduced to the structural field. Then another important kind of load is to be determined.

4.1. The fission swelling simulation circumstances

Based on Eqs. (23)–(26), the swelling values corresponding to different burnup are converted to temperature increase in every time step. On the base of the temperature load already applied, through introducing the temperature increase to the nodes of fuel particles in the finite element model, the stress and displacement results under different burnup are calculated with ANSYS. The applied temperature loads corresponding to burnup 36% along Export 1 and 2 are shown as Fig. 3(a) and (b), respectively. Firstly, the swelling simulation circumstances are investigated, illustrated as Fig. 4. The swelling values of the theoretical computation and the ones from finite element computation are compared. It can be seen that the actual volume swelling from finite element computation are very close to the

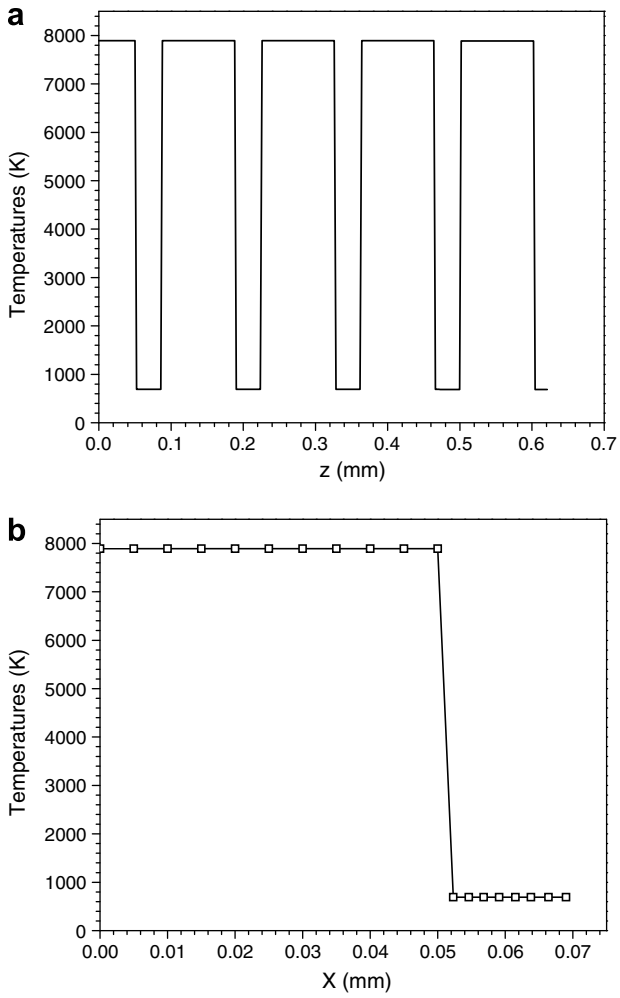

Fig. 3. The applied temperature loads corresponding to burnup 36%: (a) along export path 1, (b) along export path 2.

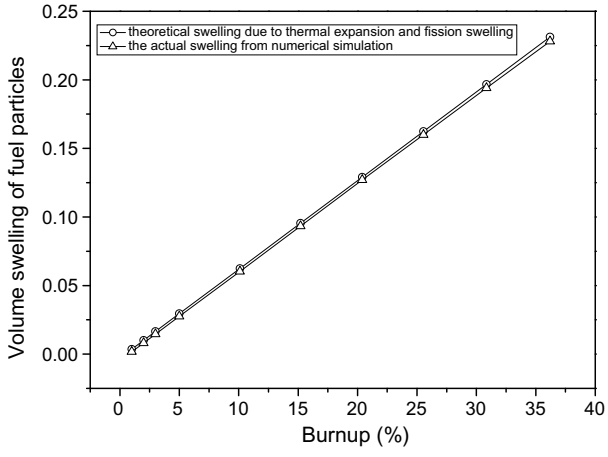

Fig. 4. The swelling comparison between the theoretical values and the ones from numerical computation.

theoretical computation ones induced by the thermal expansion and fission swelling and are slightly lower than the theoretical ones. This is because of the elastic compression strain caused by the constraint of the matrix.

4.2. Investigation of the variation of the fuel plate thickness with burnup

Fig. 5 depicts the thickness increments grow linearly with burnup. When the burnup achieves 36%, the thickness of the fuel plate rises about 6%.

4.3. The stress variation with increasing of burnup

The first principal stresses and Mises stresses along export path 1 and export path 2 are considered, as shown in Figs. 6–9.

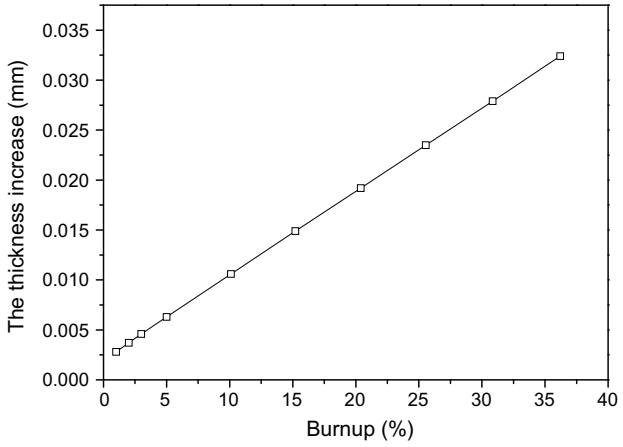

Fig. 5. The thickness increase along with burnup.

Fig. 6 denotes the variation of the first principal stresses along export path 1 with burnup. It can be found that with increasing of burnup the relative stresses at the particles change from tensile ones to compression ones and the relative tensile stresses at the matrix rise up. There exist the larger values at the places close to the interfaces between the matrix and the fuel particles, and the largest one seems to be near the interface close to the mid-plane, which might result in the failure at this region. And it can be discovered that the thermal stresses at the matrix are larger than the ones under the burnup 1%, which is caused by the fission densification at the initial stages.

Fig. 7 depicts the variation of the Mises stresses along export path 1 with burnup. It can be observed that with increasing of burnup the maximum Mises stresses at the particles transfer from the centers of the particles to the places close to the interfaces between the matrix and the particles and the maximum value increase with burnup; and for the matrix, it can be seen that the relative larger Mises stresses locate at the middle regions between the two particles; if the local plot is enlarged, it might be found that the relative larger values decrease with burnup but change slightly.

Fig. 8 illustrates the variation of the first principal stresses along export path 2 with burnup. Compared with the results shown in Fig. 7, the non-spherical symmetry of stress distribution might be discovered. It can be found that the first principal stresses at the particles decrease with burnup on the whole and the relative stresses at the matrix are negative, which means that the swelling of the fuel particles are restricted and the matrixes between the fuel particles along the length direction and the width direction are compressed. And it might also be found that at the burnup lower than 15% the abstract values of the first principal

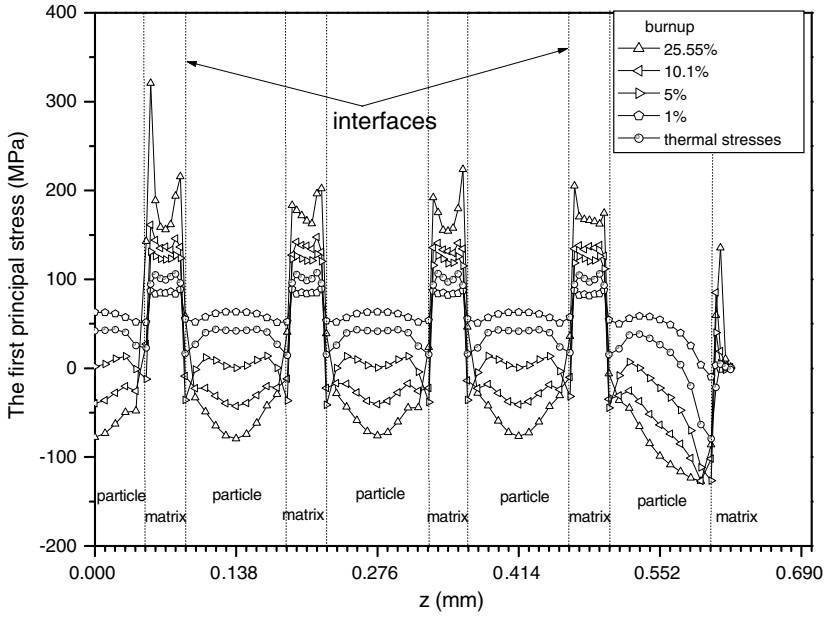

Fig. 6. The variation of the first principal stresses along the export path 1 with burnup.

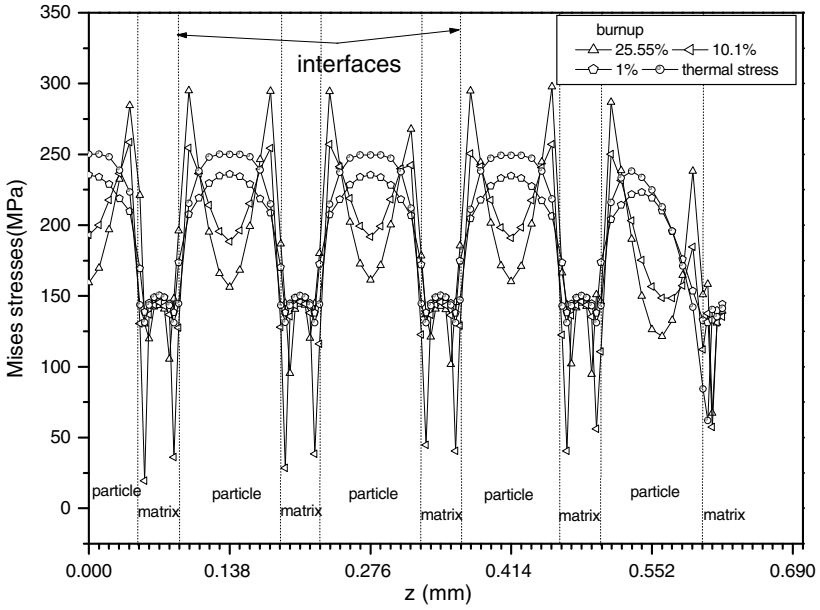

Fig. 7. The variation of the Mises stresses along the export path 1 with burnup.

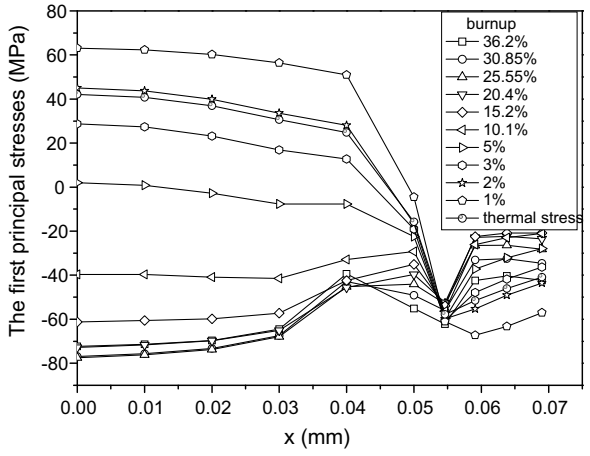

Fig. 8. The variation of the first principal stresses along export path 2 with burnup.

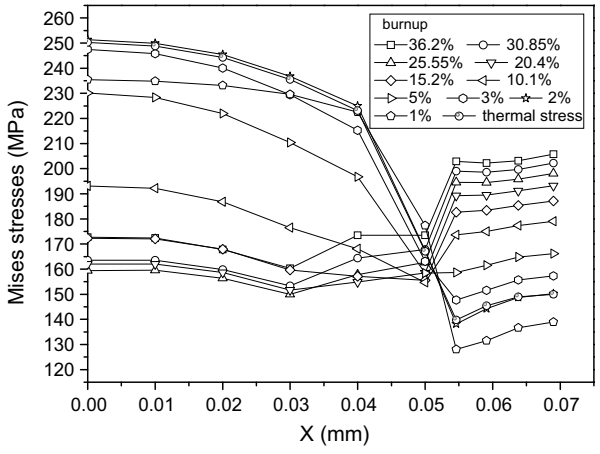

Fig. 9. The variation of the Mises stresses along export path 2 with burnup.

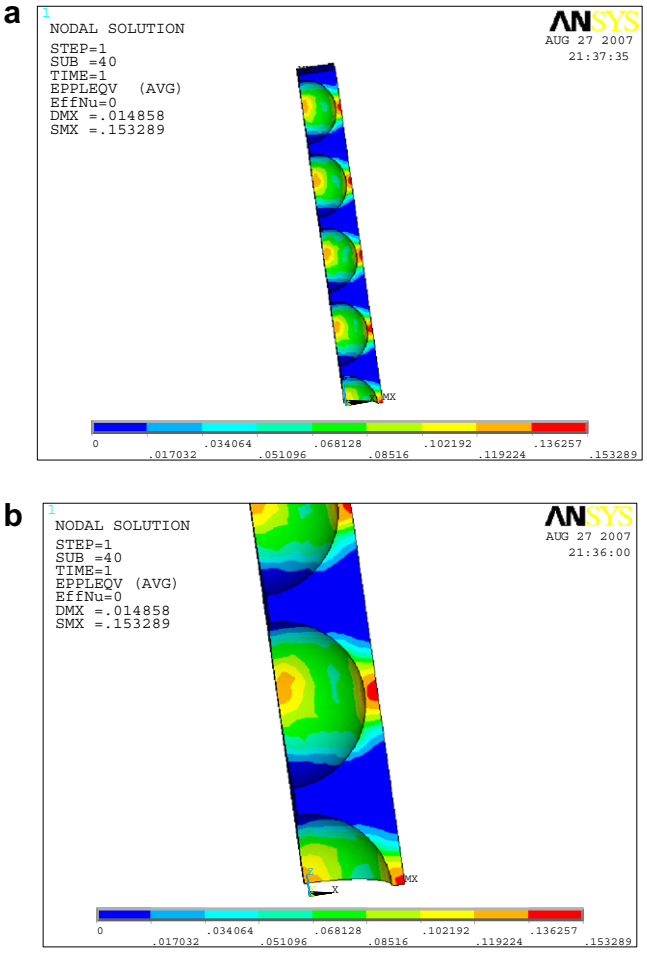

Fig. 10. The plastic strain distribution at the matrix: (a) the whole plot (b) the zoom plot.

stresses at the matrix decrease with increasing of burnup, but at the burnup larger than 15% the relative values increase with burnup.

Fig. 9 denotes the variation of the Mises stresses along export 2 with burnup. It can be observed that the maximum Mises stresses exist in the middle location of the matrix between the two particles near the mid-plane along the length direction (or the width direction). Comparing the results with the ones shown in Fig. 6, at the beginning of burnup the matrix Mises stresses at the two middle regions are almost the same, but with increasing of burnup the maximum value appears at the location mentioned above. And it can be seen from Fig. 10 that the plastic strain at the above region is also the largest.

5. Conclusions

(1) The fission swelling of fuel particles is simulated successfully by using the similarity of the fission swelling and thermal expansion.
(2) The thickness increments of the fuel plate grow linearly with burnup.
(3) The non-spherical symmetry of stress distribution is found.
(4) With increasing of burnup, the first principal stresses at the fuel particles change from tensile stresses to compression ones; the maximum Mises stresses at the particles transfer from the centers of the particles to the interfaces between the matrix and the particles, and the maximum value increase with burnup.
(5) With increasing of burnup, the first principal stresses at the matrix rise up; the maximum Mises stresses exist in the middle location of the matrix near the mid-plane between the two particles along the length direction (or the width direction). And the maximum plastic strains are also at the above region.

Acknowledgement

The authors thank for the supports of the Natural Science Foundation of China (10772049), the Natural Science Foundation of Shanghai (06ZR14009), the Pujiang Scholar Program, the Natural Science Foundation of Shanghai post-doctor.

References

[1] A.N. Holden, Dispersion Fuel Elements, Gordon and Breach Science Publishers, Inc., New York, 1967.
[2] L.V. Duyn, Evaluation of the mechanical behavior of a metal-matrix dispersion fuel for Plutonium burning, Georgia Institute of Technology: A thesis for the Degree Master of Science in Mechanical Engineering, 2003.
[3] E.A.C. Neet, K. Bakker, R.L. Belvroy, et al., J. Nucl. Mater. 317 (2003) 217.
[4] D.W. White, A.P. Beard, A.H. Willis, Irradiation behavior of dispersion fuels, paper presented at the fuels elements conference, KAPL-P-1849: Paris, 18–23 November 1957.
[5] A.G. Samoilov, A. Kashtanov, V. VOLKOV, Dispersion-fuel nuclear reactor elements, Translated from Russian, Jerusalem: Israel Program for Scientific Translations,1968.
[6] F. Lemoine, J. Nucl. Mater. 248 (1997) 238.
[7] I. Zacharie, S. Lansiart, et al., J. Nucl. Mater. 255 (1998) 92.
[8] I. Zacharie, S. Lansiart, et al., J. Nucl. Mater. 255 (1998) 85.
[9] M. Verwerft, J. Nucl. Mater. 282 (2000) 97.
[10] Donald R. Olander, Fundamental aspects of nuclear reactor fuel elements, Technical Information Center, Office of Public Affairs, Energy Research and Development Administration, 1976.
[11] C.E. Weber, H.H. Hirsch, Dispersion-Type Fuel Elements, in: International Conference on the Peaceful Uses of Atomic Energy, vol. 9, United Nations, New York, 1956, p. 196.
[12] C.E. Weber, Progress on Dispersion Elements, Progress in Nuclear Energy, Series 5, Metallurgy and Fuels, vol. 2, 1959.
[13] J. Rest, G. Hofman, Nucl. Technol. 126 (1999) 8.
[14] Z.H. Xing, S.H. Ying, Atomic Energy Sci. Technol. 35 (2001) 15.
[15] P.G. Lucuta, H.S. Matzke, I.J. Hastings, J. Nucl. Mater. 232 (1996) 166.
[16] MATPRO-09, A Handbook of Materials Properties for Use in the Analysis of Light Water Reactor Fuel Rod Behavior, USNRC TREE NUREG-1005, 1976.
[17] T. Tachibana, H. Furuya, M. Koizumi, J. Nucl. Sci. Technol. 13 (1976) 497.
[18] E.F. Fisher, C.J. Renken, Phys. Rev. (1954) A482.
[19] Motoe Suzuki et al., Nucl. Eng. Design 229 (2004) 1.
[20] W. Chubb, V.W. Storhok, D.L. Keller, Nucl. Technol. 18 (1973) 231.
[21] T. Nakajima, M. Ichikawa, et al., FEMAXI-III: A Computer Code for the Analysis of Thermal and Mechanical Behavior of Fuel Rods, AERI-1298, 1985.
[22] W. Wiesenack, M. Vankeerberghen, R. Thankappan, Assessment of UO2 Conductivity Degradation Based on In-pile Temperature Data, HWR-469, 1996.
[23] Sreedhar Kari, Harald Berger, Reinaldo Rodriguez-Ramos, Ulrich Gabbert, Compos. Struct. 77 (2007) 223.